XIV International Conference on Computational Plasticity. Fundamentals and Applications
COMPLAS 2017
E. Oñate, D.R.J. Owen, D. Peric and M. Chiumenti (Eds)

DIFFUSION-REACTION MODELLING OF THE DEGRADATION OF OIL-WELL CEMENT EXPOSED TO CARBONATED BRINE

A. MARTÍNEZ, J. LIAUDAT, C. M. LÓPEZ AND I. CAROL

ETSECCPB (School of Civil Engineering)
UPC (Technical University of Catalonia)
E-08034 Barcelona, Spain
e-mail: ariadna.martinez.e@upc.edu, joaquin.liaudat@upc.edu, carlos.maria.lopez@upc.edu, ignacio.carol@upc.edu

Key words: Carbon sequestration, Oil-well cement, CO_2, Carbonic acid, Chemical model, Finite Element Method.

Abstract. The essential aspects of a diffusion-reaction model in development for the degradation process of oil-well cement exposed to carbonated brine are presented in this paper. The formulation consists of two main diffusion/reaction field equations for the concentrations of aqueous calcium and carbon species in the hardened cement paste pore solution, complemented by a number of chemical kinetics and chemical equilibrium equations. The volume fraction distribution of the solid constituents of the hardened cement paste and the reaction products evolve with the progress of the reaction, determining the diffusivity properties of the material. A sensitivity analysis of some parameters of the model is presented to illustrate the capabilities to reproduce realistically some aspects of the degradation process.

1 INTRODUCTION

Geological storage of carbon dioxide (CO_2) is considered a promising solution to the global warming arising from anthropogenic CO_2 emissions, by capturing CO_2 from industrial and energy-related sources, transporting it usually by pipelines and injecting it into suitable deep rock formations [1]. Among other options, the storage of CO_2 in depleted oil and gas reservoirs is distinguished as one of the most favourable options; first, because the oil and gas that originally accumulated in traps did not escape, in some cases for many millions of years, demonstrating the integrity and safety of the storage site, and second, because these structures are well known and significant infrastructures are already in place at those sites. However a major source of concern arises when the security of exhausted oil fields is assessed for CO_2 storage: the presence of abandoned wells that perforate the caprock of the reservoir and which may potentially constitute CO_2 leakage pathways [2]. In particular, attention needs to be paid to the chemical stability of the cementations of those wells in the case they are exposed to carbonic acid formed by CO_2 injections. Since in most cases the construction and sealing of existing wells were not conceived taking into account future CO_2 storage, they were executed using ordinary Portland cement, which is chemically unstable in acid environments [3-8]. In this context, it becomes essential for practitioners the availability of accurate numerical

models in order to assess the long term performance of the cementation of abandoned wells in case of being exposed to new, acidic, environment due to CO_2 injections.

In this paper, a chemical model under development for simulating cement paste degradation when exposed to acidic solutions [9] is summaries together with some examples of applications. In this model the emphasis has been made on capturing the most significant chemical mechanisms that control the kinetics of the cement degradation, while keeping the formulation as simple as possible. In order to illustrate the capability of the model to reproduce realistically some aspects of the degradation process, the model was used to simulate experimental results found in the literature. Additionally, a sensitivity analysis of some model parameters is presented.

2 THE MODEL

2.1 Reaction mechanism considered

The proposed reaction mechanism is schematically summarized in Fig.1, which represents the interfacial zone between the hardened cement paste (HCP) and carbonated brine in the reservoir. The HCP is considered to be composed by four volumetric fractions: portlandite, calcium silicate hydrates (C-S-H), inert cement hydration products, namely aluminate and sulfate compounds, and capillary pores. The HCP pores are assumed to be fully saturated with water with concentrations of alkalis (sodium and potassium) and chlorides resultant from the cement hydration and from the exchange with the surrounding medium. These conditions, as well as the system pressure and temperature, are assumed to remain constant at all times during the reaction. For the sake of simplicity, C-S-H is assumed to have a fixed stoichiometry of $C_{1.7}SH_{3.2}$ (in cement chemistry notation). Then, it is decomposed in two parts, on one hand portlandite and, on the other, low calcium C-S-H, i.e. $C_{1.7}SH_{3.2}$=0.7CH + $CSH_{2.5}$. For all purposes, the portlandite in the C-S-H is treated as the rest of portlandite in the HCP.

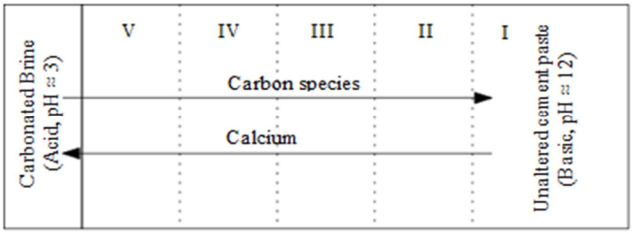

Figure 1: Scheme of the proposed degradation mechanism.

When CO_2 is dissolved in brine, carbonic acid (H_2CO_3) is formed, which is subsequently dissociated into HCO_3^- and CO_3^{2-}. This process is summarized in two Reactions (Eqs. (1) and (2)), where the intermediate formation of H_2CO_3 is omitted. The concentration gradient of carbon species causes a diffusion process from the brine towards the HCP, which is followed by a decrease of the pH of the pore solution in the HCP. As pH lowers, the portlandite in contact with the pore solution (zone II, Fig.1) becomes unstable dissolving into Ca^{2+} (Eq. (3), towards right). While there is portlandite in contact with the pore solution, the pH will remain high, and the predominant species of aqueous carbon will be CO_3^{2-}, which in turn will react

with Ca^{2+} resulting from portlandite dissolution forming calcite ($CaCO_3$) (zone III, Fig.1), as it is indicated in Eq. (4), towards left. If carbon species continue entering, the portlandite will be eventually exhausted. Consequently, the pH will decrease dissolving the calcium present in the $CSH_{2.5}$ (Eq. (5), towards right), and slowing down but not stopping the formation of calcite (zone IV, Fig.1). Additional ingress of carbon species will induce further reduction of the pH, driving calcite dissolution (Eq. (4), towards right), and continuing with the dissolution of the remaining calcium in the $CSH_{2.5}$, leaving only amorphous silicate hydrates, which are assumed to be stable in contact with the carbonated brine (zone V, Fig.1). At this stage, HCP is completely degraded with practically no mechanical strength and with high permeability.

In this processes the evolution of the solid volumetric fractions will determine important variations of the microstructure of the cement paste. In particular, the porosity of the degraded zone II is much higher than that of the unaltered cement paste. In contrast, the precipitation of calcite will reduce the porosity, in some cases, below the original value.

$$\mathrm{CO_{2\,(aq)}} + \mathrm{H_2O} \leftrightarrow \mathrm{HCO_3^-} + \mathrm{H^+} \tag{1}$$

$$\mathrm{HCO_3^-} \leftrightarrow \mathrm{CO_3^{2-}} + \mathrm{H^+} \tag{2}$$

$$\mathrm{Ca(OH)_{2\,(s)}} \leftrightarrow \mathrm{Ca^{2+}} + 2\mathrm{OH^-} \tag{3}$$

$$\mathrm{CaCO_{3\,(s)}} \leftrightarrow \mathrm{Ca^{2+}} + \mathrm{CO_3^-} \tag{4}$$

$$[\mathrm{Ca(OH)_2}][(\mathrm{SiO_2})(\mathrm{H_2O})_{1.5}] \leftrightarrow \mathrm{Ca^{2+}} + 2\mathrm{OH^-} + (\mathrm{SiO_2})(\mathrm{H_2O})_{1.5\,(s)} \tag{5}$$

$$\mathrm{H_2O} \leftrightarrow \mathrm{OH^-} + \mathrm{H^+} \tag{6}$$

2.2 Formulation

Assuming that the diffusion of aqueous species in the pore solution obeys Fick's diffusion law, averaging it in the saturated porous medium and posing the corresponding mass balance equation, the following diffusion-reaction equations for the continuum porous medium are obtained

$$\begin{cases} \dfrac{\partial(\phi c^{ca})}{\partial t} = \boldsymbol{\nabla}(D^{ca}\boldsymbol{\nabla}c^{ca}) + q^{ca} \\ \dfrac{\partial(\phi c^{tc})}{\partial t} = \boldsymbol{\nabla}(D^{tc}\boldsymbol{\nabla}c^{tc}) + q^{tc} \end{cases} \tag{7}$$

where the superscripts *ca* and *tc* indicate calcium and total carbon, respectively; ϕ is the total porosity; c^{β} [mol/m^3] is the concentration of aqueous β-species in the pore solution; D^{β} [m^2/s] is the effective diffusivity of aqueous β-species in the porous medium (assumed isotropic) and q^{β} [mol/(m^3·s)] is the rate of production/consumption of β-species per unit volume of porous medium, which in turn is a function of the concentration of aqueous calcium and total carbon, i.e. $q^{\beta} = q^{\beta}(c^{ca}, c^{ct})$. Finally, $\boldsymbol{\nabla} = [\partial/\partial x \;\; \partial/\partial y]^T$. The variable c^{tc} represents the summation of the molar concentrations of the different carbonic species in pore solution, i.e. $c^{tc}=c^{c0}+c^{c1}+c^{c2}$, where the superscript *c0* stands for $CO_{2(aq)}$, *c1* for HCO_3^- and *c2* for CO_3^{2-}.

Expressions of the production rate of calcium and total carbon are given in Eqs. (8) as functions of the net rate of production of solid species resultant from Reactions (3), (4) and

(5), where Γ^{α} [mol/(m^3·s)] is the reaction rate of solid α-species per unit volume of pore solution and superscripts CH, $C\bar{C}$ and CSH stands for portlandite, calcite and $CSH_{2.5}$.

$$q^{ca} = -\phi\left(\Gamma^{CH} + \Gamma^{C\bar{C}} + \Gamma^{CSH}\right)$$
$$q^{ct} = -\phi\left(\Gamma^{C\bar{C}}\right) \tag{8}$$

The calculation of the sink/source terms q^{β} according to Eqs. (8) requires establishing the kinetic laws for Reactions (3), (4) and (5) in order to obtain the corresponding Γ^{α}. To do so, it is assumed that the driving force of the dissolution/precipitation reaction of reactive solid α-species is (ψ^{α}-1), where ψ^{α} is the dimensionless saturation index of the pore solution with respect to the solid α-species. The saturation indexes are calculated in terms of the activity of the aqueous β-species intervening in the formation of the solid species. Activity and concentrations are related by means of dimensionless factors γ^{β} (activity coefficients), which are calculated using the well-known Davis Equation with the modification on the second term proposed by Samson and Lemaire [10]. In order to determine the concentration of secondary species, additional calculations need to be performed considering the equilibrium equations of the dissociation Reactions (1), (2) and (6), as well as, the electric charge neutrality of the pore solution. In these calculations, the concentration of other species present in the pore solution (such as alkalis or chlorides) but not intervening in Reactions (1) to (6) may be considered.

If $\psi^{\alpha} > 1$ the solution is oversaturated with respect to α-species, consequently, the reaction progresses in the precipitation direction. If $\psi^{\alpha} < 1$, the solution is under-saturated and solid dissolution occurs. If $\psi^{\alpha} = 1$, the solid and the solution are in thermodynamically equilibrium. The resulting kinetic law is formulated for a generic solid α-species in Eq.(9), where k_f^{α} and k_d^{α} [mol/(m^3·s)] are kinetic constants to be fitted and N^{α} [mol/m^3] is the concentration of solid α-species.

$$\Gamma^{\alpha} = \begin{cases} k_f^{\alpha}(\psi^{\alpha} - 1) & if\ \ \psi^{\alpha} \geq 1 \\ k_d^{\alpha}(\psi^{\alpha} - 1) & if\ \ \psi^{\alpha} < 1\ ;\ N^{\alpha} > 0 \\ 0 & if\ \ \psi^{\alpha} < 1\ ;\ N^{\alpha} = 0 \end{cases} \tag{9}$$

The mass balance equation of solid α-species is given by

$$\frac{\partial(\mathcal{U}N^{\alpha})}{\partial t} = \phi\mathcal{U}\Gamma^{\alpha} \tag{10}$$

where $\phi\mathcal{U}$ is the volume of pore solution and $\mathcal{U}$ [m^3] is the total volume of porous medium.

The total volume balance equation is given in Eq. (11), where ω^{α} [m^3/mol] is the apparent molar volume of solid α-species, and $\mathcal{U}^{cp}$[m^3] is the capillary porosity, i.e. the part of material volume that is not occupied by the solid phases and which is assumed to be filled with free water. Additionally, the total volume of pore solution includes also gel water present in gel-like solids such as C-S-H.

$$\mathcal{U} = \mathcal{U}^{cp} + \sum_{\alpha} \omega^{\alpha} M^{\alpha} \tag{11}$$

The effective diffusivity of the β-species in water-saturated HCP (D^{β}) is calculated by means of the analytical formula proposed by Oh and Jang [11] given in Eqs.(12), where D_0^{β} [m^2/s] is the diffusivity of the β-species in bulk water. This equation uses four constant dimensionless parameters which characterize the microstructure of the HCP, namely the capillary porosity (ϕ^{cp}), the percolation threshold (ϕ_c), the normalized diffusivity of the solid phase (D_s^{β}/D_0^{β}) and the percolation exponent (n). In order to introduce the effect of C-S-H dissolution in the reduction of the tortuosity of the pore structure, instead of considering n as constant, an additional expression is introduced (Eq. (13)), where n_i and n_f are the percolation exponents for unaltered and for completely decalcified HCP, respectively, and $\mathcal{U}_i^{CSH}$ is the volume of $CSH_{2.5}$ in the unaltered HCP.

$$\frac{D^{\beta}}{D_0^{\beta}} = \left(m_{\phi} + \sqrt{m_{\phi}^2 + \frac{\phi_c}{1-\phi_c}\left(\frac{D_s^{\beta}}{D_0^{\beta}}\right)^{1/n}} \right)^n \tag{12a}$$

$$m_{\phi} = \frac{1}{2}\left[\left(\frac{D_s^{\beta}}{D_0^{\beta}}\right)^{1/n} + \frac{\phi^{cp}}{1-\phi_c}\left(1 - \left(\frac{D_s^{\beta}}{D_0^{\beta}}\right)^{1/n}\right) - \frac{\phi_c}{1-\phi_c} \right] \tag{12b}$$

$$n(t) = n_i - \left(n_i - n_f\right)\left(1 - \frac{\mathcal{U}^{CSH}(t)}{\mathcal{U}_i^{CSH}}\right) \tag{13}$$

2.3 Numerical implementation

The above-described formulation has been implemented in the Finite Element code DRACFLOW, in-house developed by the group of Mechanics of Materials at UPC (MECMAT/UPC). This code has been previously used to model a number of durability problems in concrete such as drying shrinkage [12], external sulfate attack [13], Alkali-Silica Reaction [14] and high temperatures [15].

3 MODELLING RESULTS

The proposed diffusion-reaction model has been used for simulating one of the laboratory experiments performed by Duguid and Scherer [7] of well cement degradation due to exposure to carbonated brine. Additionally, a sensitivity study of the results to variations of the kinetic constants and to the way of calculating the effective diffusivity of the porous material has been performed.

3.1 The experiment

In their experiment, Duguid and Scherer [7] placed cylindrical cement paste samples (7.5 mm in diameter and 200 mm length, w/c ratio of 0.38) in a reactor with CO_2 saturated brine (0.5M NaCl) at 50 ºC. The samples were cured in 0.5 M NaCl brine at 50 ºC for 12 months. The carbonated brine had pH of 3.7 at 20 ºC and was continuously renovated in order to keep the boundary conditions as constant as possible. The evolution of the degradation front was followed by cutting small samples from the cement paste cylinder in the reactor at different times throughout the experiment. On these samples, visual measurements of depth of advance of different degradation fronts were performed.

3.2 Model geometry and parameters

The cylindrical sample has been simulated as a 1D axisymmetric problem, i.e. only radial diffusion in the sample is considered. The sample radius of 3.75 mm was discretized with 50 equal size linear finite elements. All simulations were performed for a total time of 720 hours (30 days) discretized in increments of 0.2 hours. The total carbon concentration in the carbonated brine surrounding the cement sample was estimated by means of additional calculations, as 46 mmol/L, while the concentration of calcium in the brine was assumed to be zero. Given the extended period of curing, the initial concentrations of alkalis (sodium) and chlorides were assumed homogeneous in the sample and equal to that of the brine, i.e. $c^r = c^{cl} =$ 500 mmol/L. The initial calcium concentration in pore solution is given by the equilibrium concentration of portlandite in contact with 0.5 M NaCl brine at 50 ºC, resulting in 20.95 mmol/L.

The initial concentration of the solid compounds was estimated based on the work of Brouwers [16-17] leading to the following volume fractions: $CSH_{2.5}$= 0.212, CH= 0.214, Inert cement paste= 0.220 and Capillary pores= 0.353. The total porosity (considering gel water) resulted in 0.48.

The saturation product constants considered for Reactions (3), (4) and (5) are K_{sp}^{CH}= 3.236E-06, $K_{sp}^{C\bar{C}}$= 2.007E-09 and K_{sp}^{CSH}= 3.236E-09, for activities in mol/L. The equilibrium constants considered for Reaction (1), (2) and (6) are K_{eq}^{c0}= 5.171E-07, K_{eq}^{c1}= 6.748E-11, and K_{eq}^{w}= 5.352E-14, also for activities in mol/L.

The remaining parameters (kinetic constants and diffusivity parameters) are used in the sensitivity analysis and, therefore, are indicated below for each simulated case.

3.3 Results

3.3.1 Reference case

In order to quantify the rate of progress of the degradation process, Duguid and Scherer [7] visually identified in samples taken from the cement cylinders, rings with different coloration, which were associated with different stages in the degradation process. In particular, a white ring developed in between the interior of the specimen and the practically completely decalcified outer corona. This white layer has been attributed to the presence of calcite. Then, in order to compare the measurements by Duguid and Scherer with our simulation results, the whitish color is related to a certain threshold content of calcite (0.22 m^3/m^3).

In Fig. 2, left, calcite profiles at different exposure times are plotted together. It can be appreciated how the precipitated calcite formed a relatively narrow layer that "moves" towards the interior of the sample. In the same plot, it is also indicated the adopted threshold content of calcite above which the material becomes whitish. From this plot the depths of the inner and outer sides of the whitish layer for each exposure time are obtained and plotted together with the experimental results obtained by Duguid and Scherer in Fig. 2, right. Note that the penetration rates of both the inner and the outer sides of the white layer are well reproduced by the model.

The kinetic constants used in this simulation were: $k_f^{C\bar{C}}$=5.00E-02, $k_d^{C\bar{C}}$=5.00E+02, k_d^{CH}= 1.00E+02, and k_d^{CSH}= 2.00E+01, in all cases expressed in mol/(m^3·s). The parameters used for the calculation of the effective diffusivity with Eqs. (12) and (13) were: n_i= 2.7, n_f=0.1, ϕ_c= 0.18, D_s^β / D_0^β=1.00E-04, D_0^{ct}=3.201E-09 m^2/s, and D_0^{ca}=1.327E-09 m^2/s.

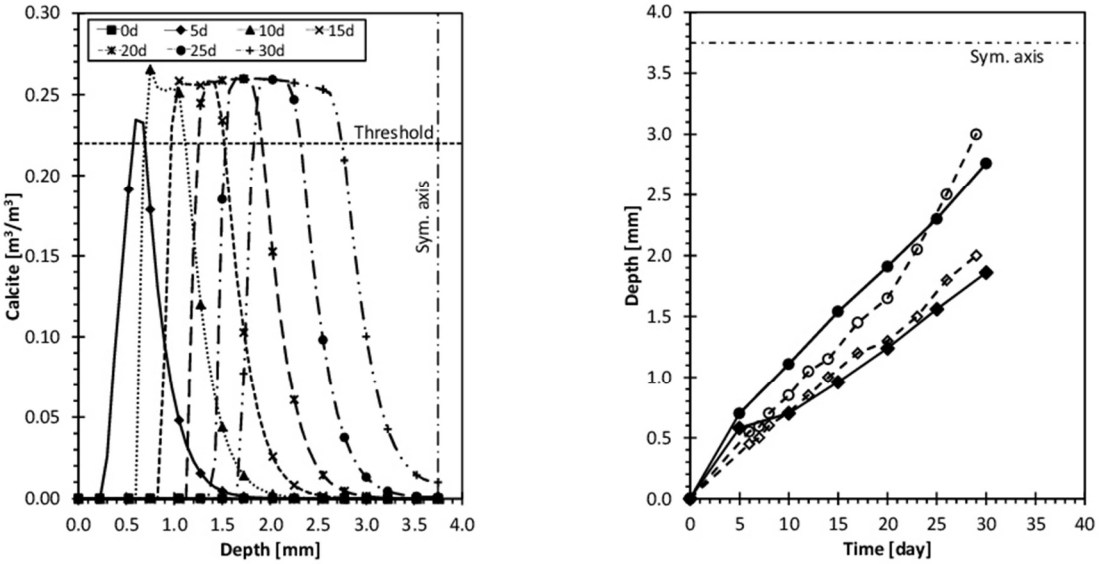

Figure 2: Left, radial profile of calcite volume fraction for different exposure times. Right, experimental and simulated reaction depth versus time. Circles and diamonds indicate the inner and the outer limits of the white layer of the degradation front, respectively. Empty symbols indicate experimental results by Duguid and Scherer [7], while solid symbols indicate simulation results.

3.3.2 Sensitivity analysis

In order to assess the influence of some parameters and modelling assumptions in the simulation results presented in previous Section 3.3.1, additional simulations were performed. In the first analysis, presented in Fig. 3, effective diffusivity was calculated in three different manners: (a) constant througout the simulation; (b) evolving as a function of capillary porosity using Eqs. (12) proposed by Oh and Jang; (c) using the formula proposed by Oh and Jang plus an evolution law, Eq. (13) for the percolation exponent. Note that (c) is the Reference case.

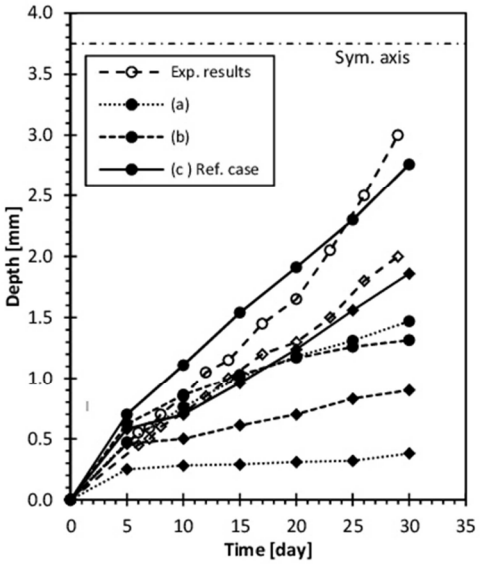

Figure 3: Experimental and simulated reaction depth versus time. The simulation results corresponds to three different maners of considering the effective diffusivity: (a) constant througout the simulation; (b) evolving as a function of capillary porosity using the formula proposed by Oh and Jang [11]; (c) using the formula proposed by Oh and Jang [11] plus an evolution law for the percolation exponent.

The rate of advancement of the reaction fronts obtained with constant diffusivity, case (a), markedly decreases with the penetration depth and clearly diverging from the experimental results. This can be explained by the growing distance to the boundary of the specimen from where the CO_2 is coming. This effect is not as marked in the experimental curves, indicating that it was somehow compensated by other mechanism. One possibility is that the increment of diffusivity due to the degradation of material compensated the greater distance to the boundary. In order to introduce this effect, a first intent was made using the formula proposed by Oh and Jang (case (b) in Fig. 3). As a result, the penetration rate of the outer front increases significantly, but the curve of the inner front remains practically unchanged. It seems that the increment of diffusivity given by the Oh and Jang formula in the degraded material was not high enough to fit the experimental results. Then, a second attempt was made introducing Eq. (13) with the intention of magnifying the effect of cement degradation on the effective diffusivity, resulting in the much better fitting of the curves of case (c).

In a second sensitivity analysis, the influence of the kinetic constants on the results obtained from the Reference case was assessed. To do so, eight additional simulations were performed. In each case, only the value of one kinetic constant was varied with respect to the one used in the Reference case. In Fig. 4, reaction depth-time curves obtained from these additional simulations are plotted together with the experimental curves and with the curves from the Reference case. The values of the corresponding modified kinetics constants are indicated in the legend of the plots.

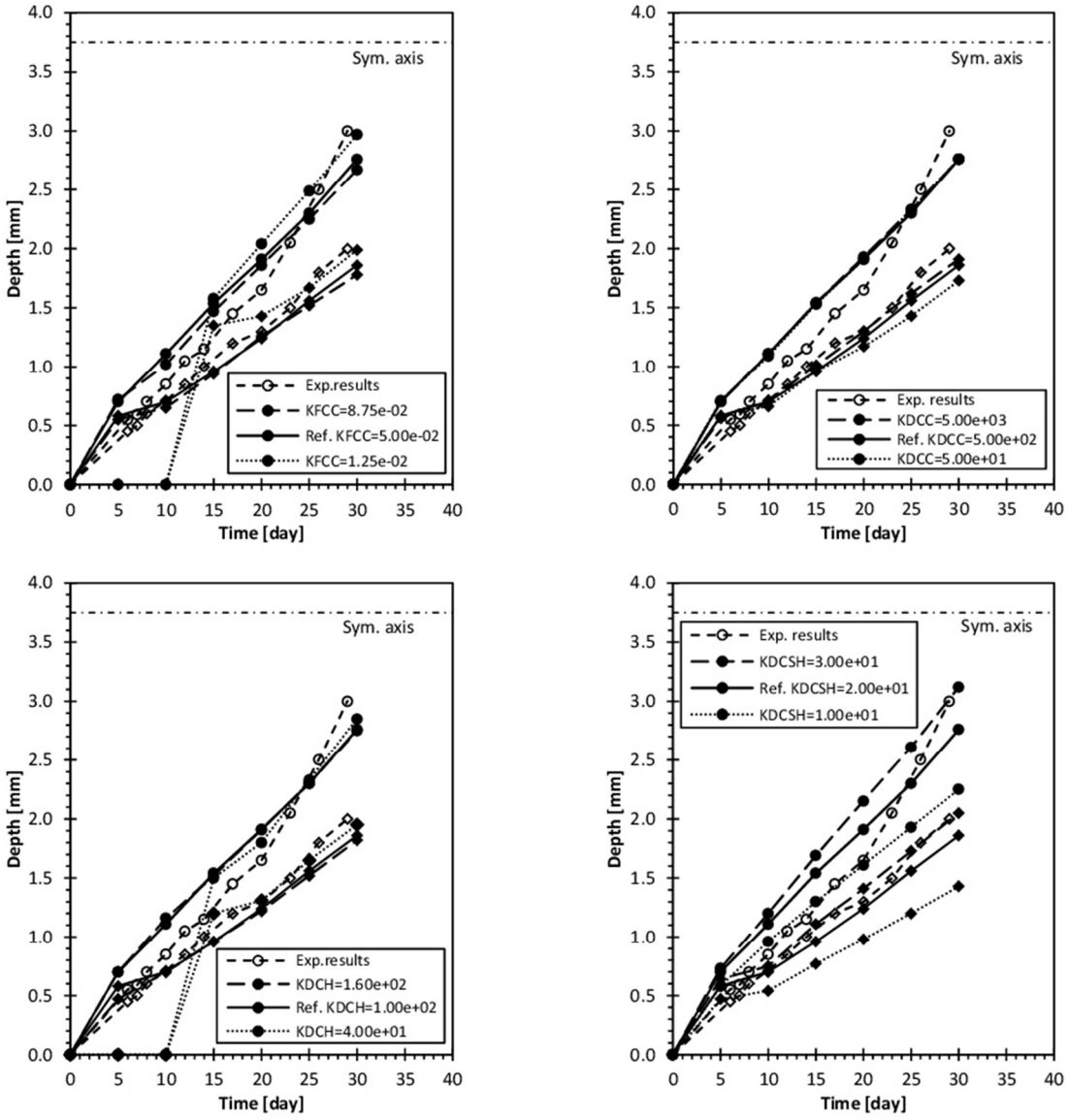

Figure 4: Experimental and simulated reaction depth versus time for the sensivity study of kinetics constants.

In the upper left plot of Fig. 4, the effect of modifying the kinetic constant of calcite formation $k_f^{C\bar{C}}$ has been represented. When $k_f^{C\bar{C}}$ is reduced, the volume of calcite formed in the first 10 days stays below the threshold value. Afterwards, the amount of calcite surpasses the adopted threshold, showing that the rate of advancement of the degradation front has not been reduced with respect to the Reference case, but slightly increased. On the other hand, increasing $k_f^{C\bar{C}}$ leads to practically the same curves as the Reference case. These results indicate that $k_f^{C\bar{C}}$ determines the peak value of the calcite radial profile, and may have also some influence on the advancement rate of the degradation fronts.

In the upper right plot of Fig. 4, the effect of modifying the kinetic constant of calcite dissolution $k_d^{C\bar{C}}$ has been represented. As expected, only the position of the outer degradation front, corresponding to the dissolution of the calcite layer, is affected by $k_d^{C\bar{C}}$. When $k_d^{C\bar{C}}$ is reduced, the dissolution of calcite is delayed and, consequently, the width of the white layer is increased. Inversely, when $k_d^{C\bar{C}}$ is increased, the width of the white layer is reduced.

In the bottom left plot of Fig. 4, the effect of modifying the kinetic constant of portlandite dissolution k_d^{CH} has been represented. As it occurs when k_d^{CH} is reduced the volume of calcite formed in the first 10 days stays below the threshold value. These results indicate that k_d^{CH} determines the peak value of the calcite radial profile but not the advancement of the degradation fronts.

In the bottom right plot of Fig. 4, the effect of modifying the kinetic constant of $CSH_{2.5}$ dissolution k_d^{CSH} has been represented. When k_d^{CSH} is increased both the inner and the outer advancement rates are increased. Inversely, when k_d^{CSH} is decreased both the inner and the outer advancement rates are decreased. This effect is more important for the inner degradation front than for the outer one and, hence, the width of the white layer increases with increasing k_d^{CSH}. The significant influence of k_d^{CSH} in the advancement of the degradation fronts is attributed to the role played by the volume fraction of $CSH_{2.5}$ in the calculation of effective diffusivity (see Eqs. (12) and (13)).

4 CONCLUDING REMARKS

- A general description of quantitative diffusion-reaction model for the simulation of cement paste degradation due to the exposure to carbonated brine has been presented.
- The proposed model seems capable of reproducing the rate of advancement of the degradation fronts.
- In order to fit experimental results, it was essential to introduce the effect of the material decalcification in the evolution of the effective diffusivity of the porous medium.
- A sensitivity analysis indicate that the kinetic constants mainly determine the width of the degradation front, with minor effect on the advancement rate, except for the dissolution kinetic constant of $CSH_{2.5}$ due to its relationship with the manner in which the effective diffusivity is calculated.
- More details of the work presented in this paper can be found in [9].

ACKNOWLEDGMENTS

This research has been supported by MEC (Madrid) through project BIA2016-76543-R which includes European FEDER funds, and by AGAUR/Generalitat de Catalunya (Barcelona) through project 2014SGR-1523. The first author also acknowledges AGAUR (Barcelona) for her FI doctoral fellowship.

REFERENCES

[1] Metz, B., Davidson, O., de Coninck, H., Loos, M., Meyer, L. & Working Group III of the Intergovernmental Panel on Climate Change (IPCC). *Carbon dioxide capture and storage* (2005).

[2] Gasda, S.E., Bachu, S., Celia, M.A. The potential for CO_2 leakage from storage sites in geological media: analysis of well distribution in mature sedimentary basins. *Environmental Geology* (2004) **46**: 6-7.
[3] Kutchko, B.G., Strazisar, B.R., Dzombak, D.A., Lowry, G.V., Thauiow, N. Degradation of well cement by CO_2 under geologic sequestration conditions. *Environmental Science and Technology* (2007) **41**: 4787-4792.
[4] Kutchko, B.G., Strazisar, B.R., Lowry, G.V., Dzombak, D.A., Thauiow, N. Rate of CO_2 Attack on Hydrated Class H Well Cement under Geologic Sequestration Conditions. *Environmental Science and Technology* (2008) **42**: 6237-6242.
[5] Rimmelé, G., Barlet-Gouédard, V., Porcherie, O., Goffé, B., Brunet, F. Heterogeneous porosity distribution in Portland cement exposed to CO_2-rich fluids. *Cement and Concrete Research* (2008) **38**: 1038-1048.
[6] Carey, J.W., Wigand, M., Chipera, S.J., WoldeGabriel, G., Pawar, R., Lichtner, P.C., Wehner, S.C., Raines, M.A., Guthrie, G.D. Analysis and performance of oil well cement with 30 years of CO_2 exposure from SACROC Unit, West Texas, USA. *International Journal of Greenhouse Gas Control* (2007) **1**: 75-85.
[7] Duguid, A., Scherer, G.W. Degradation of oilwell cement due to exposure to carbonated brine. *International Journal of Greenhouse Gas Control* (2010) **4**: 546-560.
[8] Duguid, A., Radonjic, M., Scherer, G.W. Degradation of cement at the reservoir/cement interface from exposure to carbonated brine. *International Journal of Greenhouse Gas Control* (2011) **5**: 1413-1428.
[9] Liaudat, J., Martínez, A., López, C.M., Carol, I. Modelling acid attack of oilwell cement exposed to CO_2 sequestration. *Submitted for publication.*
[10] Samson, E., Lemaire, G. Modeling chemical activity effects in strong ionic solutions. *Computational Materials* (1999) **15**: 285-294.
[11] Oh, B.H., Jang, S.Y. Prediction of diffusivity of concrete based on simple analytic equations. *Cement and Concrete Research* (2004) **34**: 463-480.
[12] Idiart, A.E., López, C.M., Carol, I. Modeling of drying shrinkage of concrete specimens at the meso-level. *Materials and Structures* (2011a) **44**: 415-435.
[13] Idiart, A.E., López, C.M., Carol, I. Chemo-mechanical analysis of concrete cracking and degradation due to external sulfate attack: A meso-scale model. *Cement and Concrete Composites* (2011b) **33**: 411-423.
[14] Liaudat, J., López, C.M., Carol, I. Numerical and Experimental study of ASR in concrete at the meso-level, in Saouma, V., Bolander, J., Landis, E. (Eds.). *The 9th International Conference on Fracture Mechanics of Concrete Structures (FraMCos 9)* (2016).
[15] Rodriguez, M., López, C.M., Carol, I. Modeling of Heat and Mass Transfer Induced by High Temperature in Concrete, in: Oñate, E., Owen, D.R.J., Peric, D., Chiument, M. (Eds). *XIII International Conference on Computational Plasticity. Fundamentals and Applications COMPLAS XIII* (2015) 346-353.
[16] Brouwers, H.J.H. The work of Powers and Brownyard revisited: Part 1. *Cement and Concrete Research* (2004) **34**: 1697-1716.
[17] Brouwers, H.J.H. The work of Powers and Brownyard revisited: Part 2. *Cement and Concrete Research* (2005) **35**: 1922-1936.